Making Aromatic Phosphorus Heterocycles More Basic and Nucleophilic: Synthesis, Characterization and Reactivity of the First Phosphinine Selenide

Friedrich Wossidlo,[a] Daniel S. Frost,[a] Jinxiong Lin,[a] Nathan T. Coles,[a] Katrin Klimov,[a] Manuela Weber,[a] Tobias Böttcher,*[b] and Christian Müller*[a]

In memoriam of François Mathey

Abstract: The synthesis and isolation of a phosphinine selenide was achieved for the first time by reacting red selenium with 2,6-bis(trimethylsilyl)phosphinine. The rather large coupling constant of $^1J_{P,Se} = 883$ Hz is in line with a P–Se bond of high *s*-character. The σ-electron donating Me₃Si-substituents significantly increase the energy of the phosphorus lone pair and hence its basicity, making the heterocycle considerably more basic and nucleophilic than the unsubstituted phosphinine C₅H₅P, as confirmed by the calculated gas phase basicities. NBO calculations further reveal that the lone pairs of the selenium atom are stabilized through donor-acceptor interactions with antibonding orbitals of the aromatic ring. The novel phosphinine selenide shows a distinct reactivity towards hexafluoro-2-butyne, Au(I)Cl as well as *i*PrOH. Our results pave the way for new perspectives in the chemistry of phosphorus in low coordination.

Introduction

Tertiary phosphines (PR₃) readily form bonds between the phosphorus atom and various electrophilic species via the phosphorus lone pair. For instance, they can be protonated and react with alkyl halides or boranes, to form phosphonium halides and phosphine-borane adducts, respectively.[1] Moreover, phosphines can readily be oxidized with H₂O₂, elemental S₈ and grey selenium resulting in the corresponding R₃P=O, R₃P=S and R₃P=Se derivatives.[2] All these conversions are typically related to the pronounced basicity and nucleophilicity of phosphines. These properties are generally strongest in trialkylphosphines and decrease with aryl-substitution at the phosphorus atom.[3] In this respect, the $^1J_{P,Se}$ coupling constant is often evaluated to estimate the degree of the electron-donating ability of a phosphine, which correlates with its Brønsted basicity.[4] This is particularly important for the development of novel phosphorus ligands for applications in homogeneous catalysis.[5]

In contrast to classical phosphines, λ³-phosphinines (phosphabenzenes), the higher homologues of pyridines, are extremely weak bases and very poor nucleophiles. This can be attributed to the rather high 3 *s*-character of the phosphorus lone pair in C₅H₅P (**1**, Figure 1), which is much higher than the value found for the nitrogen lone pair in pyridine C₅H₅N (64% 3*s* versus 29% 2*s* character).[6] The theoretical and experimental basicity of C₅H₅P has recently been re-evaluated by Nguyen

[a] Dr. F. Wossidlo, D. S. Frost, J. Lin, Dr. N. T. Coles, K. Klimov, M. Weber, Prof. Dr. C. Müller
Institut für Chemie und Biochemie
Freie Universität Berlin
Fabeckstr. 34/36, 14195 Berlin (Germany)
E-mail: c.mueller@fu-berlin.de

[b] Dr. T. Böttcher
Institut für Anorganische und Analytische Chemie
Universität Freiburg
Albertstrasse 21, 79104 Freiburg (Germany)
E-mail: tobias.boettcher@ac.uni-freiburg.de

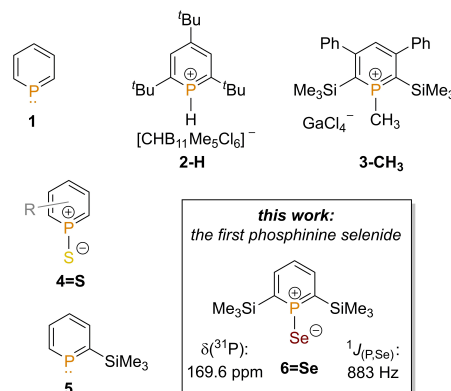📖 Supporting information for this article is available on the WWW under https://doi.org/10.1002/chem.202102390

Figure 1. Selected reactivities of the phosphorus atom in phosphinines and brief summary of this work.

et al. Values of 819.8 ± 4.2 kJ mol^{-1}, 787.5 ± 4.2 kJ mol^{-1} and -16.1 ± 1.0 were found for the gas phase proton affinity (PA), gas phase basicity (GB$_{298}$) and the pK_a of the corresponding acid C$_5$H$_5$P(H)$^+$ in aqueous solution.[7]

Nevertheless, Reed and co-workers succeeded in protonating the phosphorus atom in 2,4,6-tris-^{t}Bu-λ^3-phosphinine with the in situ generated, non-oxidizing superacid H[CHB$_{11}$Me$_5$Cl$_6$] to afford [H(C$_5$H$_2$^{t}Bu$_3$P)][CHB$_{11}$Me$_5$Cl$_6$] (**2-H**, Figure 1).[8] On the other hand, phosphinines cannot be alkylated with classical alkylating reagents, such as alkyl halides or Meerwein salts. Phosphininium salts (**3-CH$_3$**) can only be prepared via a multistep synthesis.[9] Likewise, phosphinine oxides have never been directly detected and exist only as highly reactive species.[10] Phosphinine sulfides (**4=S**) were first detected by Mathey and co-worker.[11] They are more stable than phosphinine oxides and display a high reactivity in cycloaddition reactions. A few examples of such compounds have recently been reported in the literature.[12]

Contrary to the sulfides, phosphinine selenides are still unknown. We expected that the selenation of phosphinines to be rather challenging due to the intrinsic low basicity and nucleophilicity of the phosphorus atom, which hinders the reaction with solid oligomeric or polymeric selenium species. As a matter of fact, the selenation of tertiary phosphines is usually slower than their oxidation and sulfurization, with the reaction of phosphinines with S$_8$ already requiring rather harsh reaction conditions.[12] However, we recently observed that the introduction of a Me$_3$Si-group at the α-position of the aromatic phosphorus heterocycle increases the energy of the molecular orbitals. Most notably, there is a large increase in the energy of the lone-pair in **5** (HOMO-1), with respect to the unsubstituted phosphinine **1** (HOMO-2).[13] This indicates that the phosphorus atom in **5** should show an increased basicity and nucleophilicity compared to **1** due to the σ-electron donating nature of the Me$_3$Si-group and the related β-silyl effect of this substituent. Böttcher and co-workers investigated the effect of electropositive substituents at the α-positions of pyridine and confirmed that 2,6-bis(trimethylsilyl)pyridine is much more basic than pyridine and approximately as basic in the gas phase as 4-dimethylaminopyridine (DMAP).[14] Therefore, we started a systematic study on the influence of Me$_3$Si-groups on the gas phase basicity of the corresponding phosphinines and their reactivity towards selenium. Herein we report the first synthesis and characterization of phosphinine selenides (Figure 1).

Results and Discussion

In order to obtain more information about the influence of Me$_3$Si-groups on the energetic position of the frontier orbitals and the gas-phase basicities of the corresponding P-heterocycles, we first carried out DFT calculations on selected Me$_3$Si-substituted phosphinines and the computational results are depicted in Figure 2 and listed in Table 1.[13b,15]

As expected, phosphinine **1** has a significantly lower gas phase basicity than pyridine (791.1 kJ mol^{-1} versus 898.1 kJ mol^{-1}) and the value for C$_5$H$_5$P is in excellent agreement
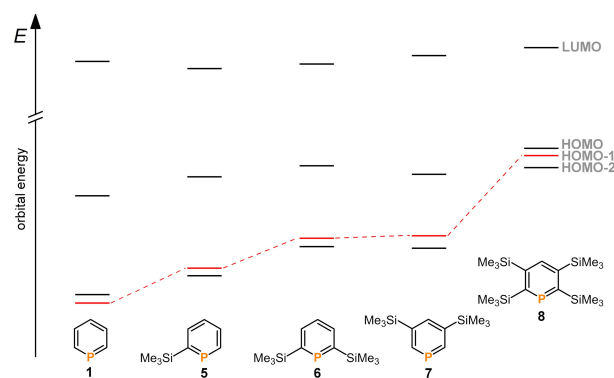

Figure 2. Frontier orbital energies of phosphinines **1** and **5–8**. Red: mainly P-lone pair.

Table 1. Electronic and thermodynamic properties of phosphinines.

Compound	LUMO energy [eV][a]	P-lone pair energy [eV][a]	Gas-phase basicity [kJ mol^{-1}][b]	δ(^{31}P) [ppm]
1	−1.510	−7.430	791.1[c]	206.4
5	−1.546	−7.258	831.9	230.7
6	−1.523	−7.071	865.8	256.1
7	−1.481	−7.056	838.4	206.4
8	−1.441	−6.581	905.5[c]	268.0

[a] B3LYP–D3/def2-TZVP level of theory. [b] DLPNO-CCSD(T)-MP2 compound method. [c] calculated gas-phase basicity of pyridine: 898.1 kJ mol^{-1}.[16]

with the literature data.[7] The gas phase basicities indeed increase considerably upon successive incorporation of Me$_3$Si-substituents. However, it seems that the influence of the position of the Me$_3$Si-groups (**6** versus **7**) on the gas phase basicity is larger than on the energetic position of the respective HOMO-1 orbitals (Figure 2).

In fact, the Me$_3$Si-group in an α-position has a greater influence on the gas phase basicity than a Me$_3$Si-group in a β-position, as also expected. On the other hand, the respective molecular orbitals (HOMO-1) are energetically almost equivalent. This discrepancy can be rationalized by comparing the shape and composition of the HOMO-1 of **6** and **7** (Figure 3).

In phosphinine **7**, the Me$_3$Si-groups in the β-position of the heterocycle are also partially involved in the HOMO-1, which is not the case in phosphinine **6**. NBO calculations indeed revealed, that the phosphorus lone pair in **6** has a 65%
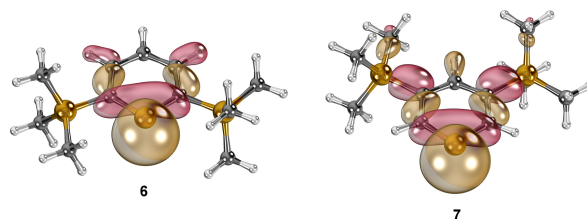

Figure 3. HOMO-1 of **6** and **7**.

contribution to HOMO-1, while in **7**, the contribution amounts to only 53%. This is perfectly in line with the calculated gas phase basicities. Among the selected phosphinines, compound **8** shows the highest value of the calculated gas phase basicities and is even more basic than pyridine in the gas phase. The calculations nicely show that the energetic destabilization of the P-lone pair and increased gas phase basicity of Me_3Si-substituted phosphinines should render species much more basic and nucleophilic than the unsubstituted phosphinine, particularly compounds **6** and **8**. This, in turn, should make those heterocycles ideal candidates for selenation reactions.

Phosphinines **1**, **5**, **6** and **8** were prepared according to literature procedures and the $^{31}P\{^1H\}$ NMR chemical shifts are listed in Table 1.[13,15] During the preparation of **8**, we noticed that this heterocycle can easily be protodesilylated at the α-position.[17] Interestingly, reaction of **8** with excess HCl in Et_2O leads selectively to phosphinine **7**, which could be isolated in high yield (Scheme 1). This allows for the synthesis of a phosphinine, which is not accessible by other routes.

Me_3Si-substituents on the aromatic phosphinine ring have only a minor influence on the position of the LUMOs, although a negative hyperconjugation, which should lower the LUMO-energy, is anticipated.[18,13] As expected (see above), introducing Me_3Si-substituents on C_5H_5P has a dramatic effect on the P-lone pair orbital energy due to their strong σ-donating properties. The change in the energetic position is most pronounced for phosphinine **8**. In this case, the P-lone pair is represented by the HOMO-1, which is also almost at the same energetic level as the HOMO. It is also significantly higher in energy than the HOMO of the unsubstituted phosphinine **1**.

In addition to the calculation of the frontier orbitals, the gas-phase basicities (GB = $-\Delta G°$ of protonation a $T = 298.15$ K) of the phosphinines depicted in Figure 2 were calculated with a high-level ab initio DLPNO-CCSD(T)-MP2 compound method (see Supporting Information for details) and the results are listed in Table 1.

Based on the reaction conditions for the synthesis of phosphinine sulfides, we first tried to react **1** with grey selenium powder in toluene at $T = 110$ °C for several days. As anticipated, no conversion towards a phosphinine selenide could be detected by means of NMR spectroscopy. In contrast, we could observe that phosphinine **5** does react with grey selenium. After several hours at $T = 100$ °C in toluene, the $^{31}P\{^1H\}$ NMR spectrum of the reaction mixture shows a new signal in addition to the resonance of the starting material. After two days under the same reaction conditions and addition of up to 10 equivalents of grey selenium, the ratio between the starting material and the product increased to about 2:1. However, excess of grey selenium or even longer reaction times had no

further effect on the conversion. The new signal showed a chemical shift at δ(ppm) = 155.5 in the $^{31}P\{^1H\}$ NMR spectrum. The chemical shift difference with respect to **5** ($\Delta\delta = 74.6$ ppm) is comparable with the value found for phosphinine sulfides ($\Delta\delta = 77.8$ ppm for 2,6-bis(trimethylsilyl)-3,5-diphenylphosphinine). The new signal shows two satellites with a coupling constant of $J = 921$ Hz, while the integral of the satellites corresponds to 8% of the total signal. Both findings are in accordance with the presence of a $^1J_{P,Se}$ coupling, while the rather large coupling constant is in line with a P–Se bond with high s-character and in the range of the value found for a phosphaalkene selenide ($^1J_{P,Se} = 890$ Hz, $Ph_3P=Se$: $^1J_{P,Se} = 736$ Hz).[4,19] This is also confirmed by the ^{77}Se NMR spectrum, which shows a doublet at δ(ppm) = 93.0 and an identical coupling constant of 921 Hz. The proton signals could be determined from a $^{31}P,^1H$-HMBC NMR spectrum. It shows that the phosphinine protons are still in the aromatic region and the ortho-trimethylsilyl substituent is still present. The NMR data suggest that a phosphinine selenide could be formed in up to 33% spectroscopic yield, but, unfortunately, it was not possible to separate **5=Se** from phosphinine **5**.

Therefore, we decided to use red selenium for the selenation reactions, as it is more reactive than grey selenium.[20] However, red selenium is thermodynamically unstable and readily converts back to grey selenium. At higher temperatures (T > 80 °C), this transformation proceeds within minutes, making the selenation reaction of phosphinines even more challenging. Red selenium was therefore reacted with **1** in CH_2Cl_2 at room temperature to prevent rapid conversion of red selenium into grey selenium (Scheme 2).

Gratifyingly, we were able to convert even **1** with a maximum spectroscopic yield of 15% to phosphinine selenide **1=Se** (Table 2). In the case of phosphinine **5**, it was possible to significantly increase the conversion to **5=Se** from 33% (grey selenium, see above) to 80% spectroscopic yield (Table 2).

However, it was not possible to achieve full conversion, even with longer reaction times or lower reaction temperatures. Much to our delight, the more nucleophilic 2,6-bis(trimethylsilyl)-phosphinine (**6**) was converted quantitatively

Scheme 2. Reaction of phosphinines with red selenium.
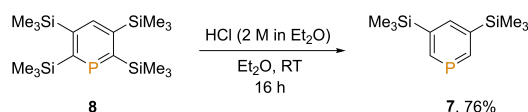
Scheme 1. Synthesis of **7** via protodesilylation of **8**.

Table 2. Spectroscopic yield and selected NMR spectroscopic data of phosphinine selenides.

Compound	Yield (%)[a]	δ(^{31}P) [ppm]	$^1J_{31P,77Se}$ [Hz]
1=Se	15	143.4	937
5=Se	80	155.5	908
6=Se	100	169.6	883
7=Se	73	144.4	917
8=Se	3	183.6	858

[a] yield based on $^{31}P\{^1H\}$ NMR spectroscopy.

Chemistry–A European Journal

Full Paper
doi.org/10.1002/chem.202102390

Chemistry
Europe
European Chemical
Societies Publishing

with red selenium to **6=Se**, according to $^{31}P\{^1H\}$ NMR spectroscopy and the pure compound was isolated in 98% yield as a slightly yellow oil. The proton-coupled ^{31}P NMR spectrum of **6=Se** is depicted in Figure 4 and shows a signal with ^{77}Se-satellites at $\delta(ppm) = 169.6$ ppm and with P-H$_{meta}$ and P-H$_{ortho}$ coupling constants of 43.1 and 7.5 Hz, respectively.

Even though the spectroscopic data indicate the successful synthesis of **6=Se**, no single crystals of this compound could be obtained so far as a final proof for its molecular structure. However, in analogy to phosphinine sulfides, we found that **6=Se** also easily undergoes [4+2] cycloaddition reactions. Upon reaction of **6=Se** with hexafluoro-2-butyne in dichloromethane at room temperature, the corresponding 1-phosphabarrelene selenide (**9**) could be obtained quantitatively and was isolated as colorless crystals in 86% yield (Scheme 3).

Crystals of **9**, suitable for X-ray crystal structure analysis, could be obtained by slow evaporation of the solvent from a
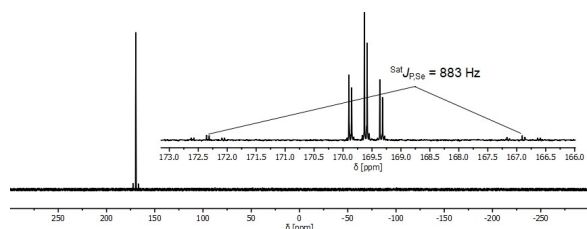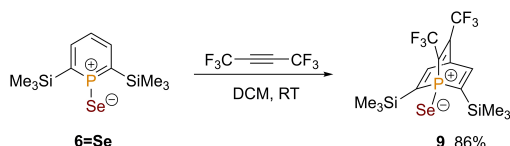
Figure 4. ^{31}P NMR spectrum of **6=Se**. Inset: enlargement of the signal region.

Scheme 3. [4+2] Cycloaddition of $F_3CC\equiv CCF_3$ to phosphinine selenide **6=Se**.
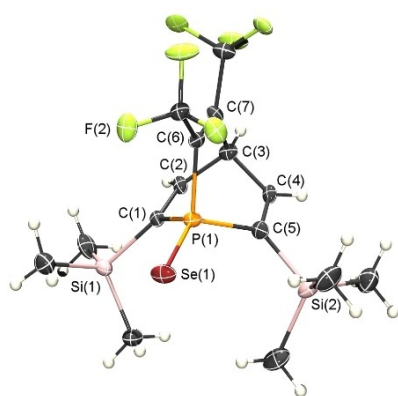
Figure 5. Molecular structure of **9** in the crystal. Displacement ellipsoids are shown at the 50% probability level. Selected bond lengths (Å) and angles (°): P(1)-Se(1): 2.0880(8); P(1)-C(1): 1.816(3); P(1)-C(5): 1.821(3); C(1)-C(2): 1.320(4); C(2)-C(3): 1.536(4); C(3)-C(4): 1.533(4); C(4)-C(5): 1.320(4); C(3)-C(7): 1.526(4); P(1)-C(6): 1.857(3); Σ ∡ (C–P-C) 296.10(14).

toluene solution. The molecular structure of **9** in the crystal, along with selected bond lengths and angles, are depicted in Figure 5.

The bond lengths and angles are in good agreement with those of other reported 1-phosphabarrelene selenides, which were obtained by direct selenation of the corresponding 1-phosphabarrelenes.[21] The crystallographic characterization of **9** provides clear evidence for the successful synthesis of **6=Se**. Having proven that phosphinine selenides are synthetically accessible, we also hoped the selenation of phosphinines **7** and **8** could be conducted under the same reaction conditions as for **6** to **6=Se**. In both cases the formation of the corresponding products **7=Se** and **8=Se** was observed, however, complete conversion was not achieved (73% spectroscopic yield for **7→7=Se**; 3% spectroscopic yield for **8→8=Se**) (Table 2).

A comparison of the P-lone pair energies (Figure 2), gas phase basicities (Table 1) and $^1J_{P,Se}$ coupling constants (Table 2) of the phosphinines and phosphinine selenides reveal a rather good correlation with respect to the reactivity of the phosphinines towards selenium. Indeed, phosphinine selenide **8=Se**, which contains the most basic phosphorus heterocycle in this series, shows the smallest $^1J_{P,Se}$ coupling constant of 858 Hz, while **1=Se**, containing the least basic unsubstituted phosphinine, shows the largest coupling constant of $^1J_{P,Se} = 937$ Hz. The lower conversion of **7** to **7=Se** compared to the reaction of **6→6=Se** can be understood in view of the slightly lower basicity/nucleophilicity of **7** compared to **6**. It should be kept in mind that a longer reaction time due to a reduced basicity/ nucleophilicity of the phosphinine is counterproductive for the selenation reaction, as the red selenium is rather rapidly converted back to the far less reactive grey selenium under the applied reaction conditions, even at room temperature. This was already observed for the conversion of phosphinine **1** to phosphinine selenide **1=Se** (15%), and respectively **5** to **5=Se** (80%). These phosphinines feature no, or only one, Me$_3$Si-group. Nevertheless, particularly surprising is the low conversion of **8** to **8=Se**, as phosphinine **8** shows the highest gas-phase basicity of the investigated phosphinines. We thus expect that steric factors also play a significant role in the interaction of the phosphorus donor with the oligomeric structures of solid red selenium. As a matter of fact, the results of the computational geometry optimizations of phosphinines **6** and **8** support the hypothesis of steric hindrance around the phosphorus atom by the Me$_3$Si-groups. The corresponding calculated bond lengths, distances and angles are depicted in Figure 6.
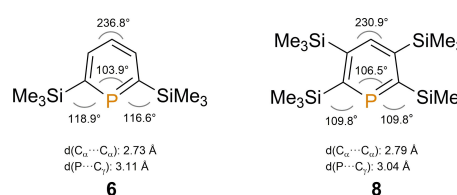
Figure 6. Calculated bond angles and distances in **6** and **8**.

Chemistry–A European Journal

Full Paper
doi.org/10.1002/chem.202102390

Chemistry Europe
European Chemical
Societies Publishing

The P-C$_{ortho}$-Si-angles are larger in **6** compared to **8**. Moreover, the four Me$_3$Si-groups in **8** cause a slight compression of the phosphorus heterocycle, as the C$_\alpha$–P–C$_\alpha$ and C$_\beta$–C$_\gamma$–C$_\beta$ angles are wider than in **6**, which also leads to a slightly smaller P-C$_\alpha$ distance in **8** with respect to **6**. The calculated geometry for **6=Se** revealed that the two Me$_3$Si-groups in the α-positions are still flexible and allow for the formation of a planar phosphinine selenide. In contrast, this is not the case for **8=Se**. The flexibility of the Me$_3$Si-groups in the α-positions are hampered by the Me$_3$Si-groups in the β-positions. As a consequence, the phosphinine ring in **8=Se** is severely distorted from the expected planarity. Accordingly, the phosphorus atom in phosphinine **8** is more basic than the phosphorus atom in phosphinine **6**, but much less nucleophilic. The different bond lengths and angles in **8** compared to **6** also have a pronounced effect on the energetic level of the respective frontier orbitals (Figure 2). In fact, the HOMO, HOMO-1 (lone pair) and HOMO-2 of **8** are disproportionately high in energy with respect to the corresponding molecular orbitals of the less-substituted phosphinines **1, 5–7**.

The analysis of the bonding in **1=Se** by means of NBO-DFT calculations revealed that lone pair 1 (LP(1)) donates electron density into two equivalent σ*(P–C) orbitals, while LP(2) donates electron density very strongly into an energetically low-lying π*(P–C) orbital (Figure 7 and Table 3). The energetic
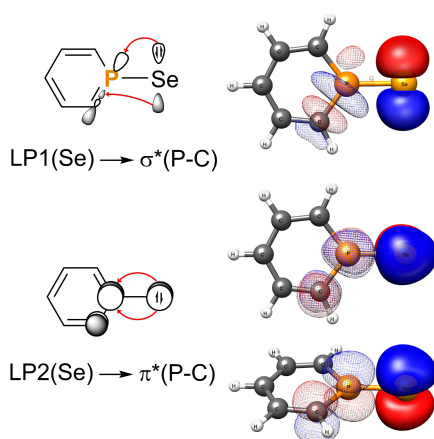
stabilization by the donor-acceptor interactions is ΣE(2) = 54.74 kcal/mol and thus, as expected, slightly smaller than the reported value for the phosphinine sulfide C$_5$H$_5$P=S (ΣE(2) = 66.52 kcal/mol).[12a] It is interesting to note that in the latter compound, the stabilization energy is almost twice as high than in phosphine sulfides R$_3$P=S.[12a] This is apparently also the case for **1=Se** and phosphine selenides. Likewise, the interaction between the two lone pairs at the selenium atom and the phosphorus atom is also clearly visualized by the shape of the intrinsic bond orbitals (IBOs) in **1=Se** (Figure 8).

The NBO-DFT calculations further demonstrated that there is no significant difference in the hybridization state of the phosphorus atom between **1=Se** and C$_5$H$_5$P=S and the s- and p-character of the corresponding P–C and P=X (X = S, Se) bonds (Table 4).

We also investigated the effect of the Me$_3$Si-substituents on the P–Se bond strengths and the results are listed in Table 5. The computational analyses are in agreement with our experimental observations. Except for the tetrakis-Me$_3$Si-functionalized phosphinine (**8=Se**), the P–Se bond strengths increase with the number of Me$_3$Si-substituents. As expected, the P–Se bond strength in **7=Se**, in which the Me$_3$Si-groups are located in the β-position with respect to the phosphorus atom, is considerably smaller than in **6=Se** (Me$_3$Si-groups in α-position). Accordingly, the charges (QTAIM analysis) at the Se-
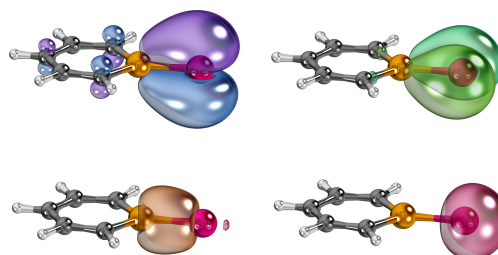

LP1(Se) ⟶ σ*(P-C)

LP2(Se) ⟶ π*(P-C)

Figure 7. NBO plots of selected donor-acceptor interactions in phosphinine selenides.

Figure 8. Selected IBOs for C$_5$H$_5$P=Se (**1=Se**).

Table 3. NBO analysis of selected donor-acceptor interactions in **1=Se** and C$_5$H$_5$P=S.[a]

Donor	Acceptor	Energy	**1=Se**	C$_5$H$_5$P=S
LP(1)	σ*(P–C)	E(2)[b]	10.87	13.51
		E_{ij}[c]	0.48	0.49
		F_{ij}[c]	0.064	0073
LP(1)	σ*(P–C)	E(2)[b]	10.59	13.51
		E_{ij}[c]	0.48	0.49
		F_{ij}[c]	0.064	0.073
LP(2)	π*(P–C)	E(2)[b]	32.99	39.50
		E_{ij}[c]	0.16	0.17
		F_{ij}[c]	0.064	0.073

[a] B3LYP–D3/def2-TZVP level of theory. [b] in kcal/mol. [c] in a.u.

Table 4. Hybridization state of the phosphorus atom in **1=Se** and C$_5$H$_5$P=S.[a]

	P–C bond			P=X bond (X = S, Se)		
	s-char. (%)	p-char. (%)	sp^λ	s-char. (%)	p-char. (%)	sp^λ
1=Se	31.9	67.8	$sp^{2.13}$	35.4	63.8	$sp^{1.80}$
C$_5$H$_5$P=S	31.7	67.9	$sp^{2.14}$	35.0	64.1	$sp^{1.83}$

[a] B3LYP–D3/def2-TZVP level of theory.

Table 5. Δ$H°$ [kJ mol^{-1}] for the reaction phosphinine + Se → phosphinine = Se and calculated charge at the selenium atom.[a]

Compound	Δ$H°$ [kJ mol^{-1}]	QTAIM charge at Se[a]
1=Se	−227.1	−0.334
5=Se	−243.1	−0.357
6=Se	−259.0	−0.375
7=Se	−233.1	−0.362
8=Se	−233.1	−0.388

[a] B3LYP/def2-TZVP-D3(BJ) level of theory.

Chemistry–A European Journal

Full Paper
doi.org/10.1002/chem.202102390

Chemistry
Europe
European Chemical
Societies Publishing

atom also increase with increasing number of Me₃Si-groups, which is perfectly in line with the increasing basicity of the phosphorus atom in going from **1=Se** to **8=Se**. These values correlate well with the $^{1}J_{P,Se}$ coupling constants (Table 2). However, the P–Se bond strength in **8=Se** is considerably smaller than expected, as this compound should show the highest value among the series **1=Se→8=Se**. Nevertheless, this discrepancy might be due to steric effects. As mentioned above, the heterocycle in **8=Se** is significantly distorted, while the loss of planarity upon selenation of the phosphorus atom takes place at the expense of the reaction enthalpy. This is also in line with the observed low yield for the formation of **8=Se**. In **6=Se**, both Me₃Si-groups in α-position can easily accommodate the selenium atom without any loss of planarity of the phosphorus-containing ring.

As we have demonstrated above, **6=Se** is cleanly and quantitatively converted with hexafluoro-2-butyne to the corresponding 1-phosphabarrelene-selenide **9** (Scheme 3). Consequently, we started to explore the reactivity of **6=Se** in more detail. First, we were interested whether **6=Se** can serve as a ligand towards Au(I), as the corresponding AuCl complex of Ph₃P=Se has been reported in literature.[22] Addition of an equimolar amount of AuCl·SMe₂ to a solution of **6=Se** in dichloromethane at room temperature leads, however, to the quantitative formation of the phosphinine-AuCl complex **10** and a grey precipitate (Scheme 4).[23] This is a clear indication that the phosphorus-selenium bond in **6=Se** is rather labile

and immediate decomposition occurs upon addition of AuCl·SMe₂.[24] This could provide interesting opportunities to use **6=Se** in selenium transfer reactions.[25]

Upon trying to crystallize **6=Se** over several weeks at $T = -80\,°C$ in a Schlenk flask suspended in *i*PrOH, crystals suitable for a crystallographic characterization were isolated. The result of the X-ray crystal structure analysis reveals, however, that *i*PrOH had been added in an *anti* fashion to the P=C double bond of **6=Se** forming product **11** (Figure 9). This is assumed to be due to very slow diffusion of *i*PrOH into the reaction flask. Relating to this, transition metal complexes of phosphinines tend to react with protic reagents, such as water or alcohols.[26] This leads to addition of the RO–H group to the P=C double bond, which is commonly facilitated when the metal center is in a higher oxidation state. Similarly, the P=C double bond in phosphinine sulfides is also prone to addition reactions in the presence of water or alcohols, as already demonstrated by us.[12b]

When trying to reproduce this observed reactivity by adding a small amount of *i*PrOH to a solution of **6=Se** in toluene at room temperature the reaction mixture showed two resonances with selenium satellites in the $^{31}P\{^{1}H\}$ spectrum at $\delta(ppm) = 87.0$ ($^{1}J_{P,Se} = 747$ Hz) and 49.5 ($^{1}J_{P,Se} = 747$ Hz), respectively, with the signals in a ratio of approximately 1:0.9. The resonance at $\delta(ppm) = 87.0$ was assigned to compound **11** based on the ^{1}H NMR spectrum, which shows two signals for the TMS groups ($\delta(ppm) = 0.28$ and 0.16) along with inequivalent isopropyl methyl groups ($\delta(ppm) = 1.36$ and 1.40). The proton adjacent to the phosphorus atom is observed at $\delta(ppm) = 2.93$, which originates from *i*PrOH, and a complicated multiplet for the isopropyl C–H is detected at $\delta(ppm) = 5.06$. Two signals for the diene protons are observed at $\delta(ppm) = 6.58$, which integrate to 1, and a multiplet between $\delta(ppm) = 6.32-6.09$, which integrates to 2. These signals are characteristic for the addition of *i*PrOH to the P=C double bond in an *anti* fashion to form compound **11**.[26]

The nature of the second species (see above) still remains unknown. Several attempts were made to grow crystals of this compound, however, only the *anti* isomer could be isolated and characterized crystallographically in each case. The unknown species shows a P–Se coupling at $\delta(ppm) = 49.5$ in the $^{31}P\{^{1}H\}$ spectrum and a Se–H coupling in the ^{1}H NMR spectrum. Therefore, we exclude that this compound is the *syn*-diastereomer of **11**. Moreover, this species appears to be unstable. In the presence of PPh₃ as an internal standard, it converts quantitatively to **11** before decomposition of the sample occurs. Unfortunately, complete characterization and structural identification of this species has not been possible.

Finally, we were interested in comparing the electrostatic potential maps of Ph₃P=Se with **6=Se** in order to get an idea on the charge distributions in these compounds and potential charge related properties and reactivities. Both compounds clearly show a σ-hole at the selenium atom (Figure 10).

Interestingly, however, the σ-hole is much more pronounced in the phosphinine selenide compared to triphenylphosphine selenide. This again can be attributed to the higher *s*-character of the P–Se bond in **6=Se** compared to the one in

Scheme 4. Reaction of **6=Se** with AuCl·SMe₂ and *i*PrOH. Only one enantiomer of **11** is shown.
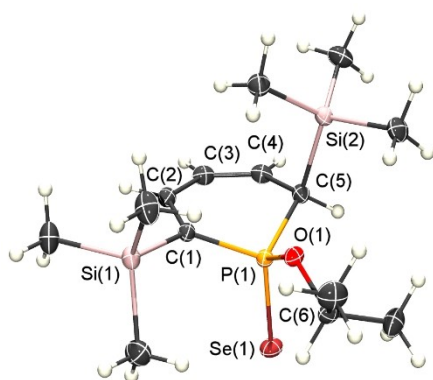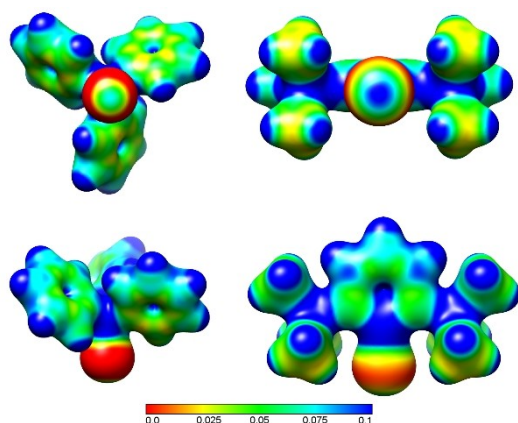
Figure 9. Molecular structure of **11** in the crystal. Displacement ellipsoids are shown at the 50% probability level. Solvent molecule omitted for clarity. Selected bond lengths (Å) and angles (°): P(1)-Se(1): 2.1054(4); P(1)-O(1): 1.6007(8); P(1)-C(1): 1.7860(12); P(1)-C(5): 1.8020(12); C(1)-C(2): 1.3575(16); C(2)-C(3): 1.4560(17); C(3)-C(4): 1.3407(17); C(4)-C(5): 1.5040(16); C(1)-Si(1): 1.8822(12); C(5)-Si(2): 1.9330(12).

Chemistry–A European Journal

Full Paper
doi.org/10.1002/chem.202102390

Chemistry
Europe
European Chemical
Societies Publishing

Figure 10. Electrostatic potential plot of Ph$_3$P=Se (left) and **6**=**Se** (right) calculated at B3LYP-D3/def2-TZVP level of theory. The electrostatic potential (in a.u.) is mapped on electron density isosurfaces of 0.02 e/au^3.

Ph$_3$P=Se. This indicates that **6**=**Se** could possibly form adducts with additional donor molecules, in which the selenium atom acts as an acceptor of a phosphorus-chalcogenide bond. So far, only adducts with phosphorus-selenides are known, in which the selenium atom acts as the donor.[27]

Conclusion

In conclusion, we could demonstrate by both theoretical calculations and reactivity studies that the very low basicity and nucleophilicity of the phosphorus donor in phosphinines can be drastically increased by introducing strongly σ-donating Me$_3$Si-substituents to the aromatic phosphorus heterocycle. The highest gas phase basicity was found for 2,3,5,6-tetrakis(trimethylsilyl)phosphinine, being even more basic in the gas phase than pyridine. This finding led to the first quantitative synthesis of a phosphinine selenide by reacting red selenium with 2,6-bis(trimethylsilyl)phosphinine. The measured phosphorus selenium coupling constant confirms that the P–Se bond in phosphinine selenides has a high s-character and that Me$_3$Si-substituted phosphinines are indeed more basic than regular phosphinines. In addition, NBO calculations show the presence of donor-acceptor interactions of the selenium lone pairs with antibonding orbitals of the phosphorus heterocycle. We further found that the charges at the Se-atom increase with increasing number of Me$_3$Si-groups, which is perfectly in line with the increasing basicity of the phosphorus atom in going from **1**=**Se** to **8**=**Se**. These values correlate well with the $^1J_{P,Se}$ coupling constants. However, the P–Se bond seems to be rather weak, as demonstrated by reaction of the phosphinine selenide with Au(I)Cl. The formation of selenides was also shown for other phosphinines, but not with complete conversion. In addition to the increased basicity, steric effects of Me$_3$Si-groups seem to influence the reaction between phosphinines and selenium considerably. The novel phosphinine selenide reacts readily with hexafluoro-2-butyne in a [4+2] cycloaddition

reaction to afford the corresponding 1-phosphabarrelene selenide selectively. In the presence of isopropanol, the facile addition of the RO–H group to the P=C double bond of the phosphinine selenide occurs. DFT calculations of the electron density distributions in phosphinine selenides further revealed the presence of a σ-hole on the selenium atom. This could lead to interesting adducts with donor molecules, with the selenium atom acting as an acceptor of a phosphorus-chalcogenide bond. We expect, that phosphinines containing strongly σ-donating substituents, will provide fascinating perspectives in the future, particularly for the synthesis of hitherto unknown adducts with main group elements and compounds. Experiments in this direction are currently performed in our laboratories.

Experimental Section

Experimental details are given in the Supporting Information. Deposition Numbers 2067304 (for **9**) and 2067303 (for **11**) contain the supplementary crystallographic data for this paper. These data are provided free of charge by the joint Cambridge Crystallographic Data Centre and Fachinformationszentrum Karlsruhe Access Structures service.

Conflict of Interest

The authors declare no conflict of interest.

Keywords: aromaticity · crystallography · density functional calculations · heterocycles · phosphinine

[1] a) A. Staubitz, A. P. M. Robertson, M. E. Sloan, I. Manners, *Chem. Rev.* **2010**, *110*, 4023–4078; b) V. Iaroshenko, *Organophosphorus Chem.*, Wiley-VCH, Weinheim, **2019**; c) M. Selva, A. Perosa, G. Fiorani, *Organophosphorus Chem.* **2019**, *48*, 145–198.

[2] a) E. I. Musina, A. S. Balueva, A. A. Karasik, *Organophosphorus Chem.* **2019**, *48*, 1–63; b) G. Keglevich, *Organophosphorus Chem.* **2019**, *48*, 103–144.

[3] a) W. A. Henderson, C. A. Streuli, *J. Am. Chem. Soc.* **1960**, *82*, 5791–5793; b) W. A. Henderson, S. A. Buckler, *J. Am. Chem. Soc.* **1960**, *82*, 5794–5800.

[4] a) D. W. Allen, B. F. Taylor, *J. Chem. Soc. Dalton Trans.* **1982**, 51–54; b) U. Beckmann, D. Süslüyan, P. C. Kunz, *Phosphorus, Sulfur, and Silicon* **2011**, *186*, 2061–2070; c) I. L. Rusakova, Y. Y. Rusakov, *Magn. Reson. Chem.* **2020**, *58*, 929–940.

[5] *Phosphorus Ligand Effects in Homogeneous Catalysis: Design and Synthesis* (Eds.: P. C. J. Kamer, P. W. N. M van Leeuwen), Wiley-VCH, Weinheim, **2012**.

[6] P. Le Floch, *Coord. Chem. Rev.* **2006**, *250*, 627–681.

[7] N.-N. Tham-Tran, G. Bouchoux, D. Delaere, M. T. Nguyen, *J. Phys. Chem. A* **2005**, *109*, 2957–2963.

[8] Y. Zhang, F. S. Tham, J. F. Nixon, C. Taylor, J. C. Green, C. A. Reed, *Angew. Chem. Int. Ed.* **2008**, *47*, 3801–3804.

[9] A. Moores, L. Ricard, P. Le Floch, *Angew. Chem. Int. Ed.* **2003**, *42*, 4940–4994; *Angew. Chem.* **2003**, *115*, 5090–5094.

[10] a) K. Dimroth, K. Vogel, W. Mach, U. Schoeler, *Angew. Chem. Int. Ed.* **1968**, *7*, 371–371; *Angew. Chem.* **1968**, *80*, 359–360; b) K. Dimroth, A. Chatzidakis, O. Schaffer, *Angew. Chem. Int. Ed.* **1972**, *11*, 506–506; *Angew. Chem.* **1972**, *84*, 526–527; c) A. Hettche, K. Dimroth, *Chem. Ber.* **1973**, *106*, 1001–1011.

[11] J.-M. Alcaraz, F. Mathey, *J. Chem. Soc. Chem. Commun.* **1984**, 508–509.

[12] a) A. Moores, T. Cantat, L. Ricard, N. Mézailles, P. Le Floch, *New J. Chem.* **2007**, *31*, 1493–1498; b) G. Pfeifer, P. Ribagnac, X.-F. Le Goff, J. Wiecko, N. Mézailles, C. Müller, *Eur. J. Inorg. Chem.* **2015**, 240–249.

[13] a) M. H. Habicht, F. Wossidlo, M. Weber, C. Müller, *Chem. Eur. J.* **2016**, *22*, 12877–12883; b) M. H. Habicht, F. Wossidlo, T. Bens, E. A. Pidko, C. Müller, *Chem. Eur. J.* **2018**, *24*, 944–952.

[14] J. Schröder, D. Himmel, T. Böttcher, *Chem. Eur. J.* **2017**, *23*, 10763–10767.

[15] N. Avarvari, P. Le Floch, F. Mathey, *J. Am. Chem. Soc.* **1996**, *118*, 11978–10979.

[16] E. P. L. Hunter, S. G. Lias, *J. Phys. Chem. Ref. Data* **1998**, *27*, 413–656.

[17] M. Blug, O. Piechaczyk, M. Fustier, N. Mézailles, P. Le Floch, *J. Org. Chem.* **2008**, *73*, 3258–3261.

[18] V. R. Ferro, S. Omar, R. H. González-Jonte, G. de la Vega, *Heteroat. Chem.* **2003**, *14*, 160–169.

[19] T. A. van der Knaap, M. Vos, F. Bickelhaupt, *J. Organomet. Chem.* **1983**, *244*, 363–367.

[20] R. Steudel, *Chemie der Nichtmetalle, Synthesen - Strukturen - Bindung - Verwendung* (de Gruyter, Berlin, ed. 4, **2014**).

[21] M. Rigo, E. R. M. Habraken, K. Bhattacharyya, M. Weber, A. Ehlers, N. Mézailles, C. Slootweg, C. Müller, *Chem. Eur. J.* **2019**, *25*, 8769–8779.

[22] M. Sakhawat Hussain, *J. Crystallogr. Spectrosc. Res.* **1986**, *16*, 91.

[23] N. Mézailles, L. Ricard, F. Mathey, P. Le Floch, *Eur. J. Inorg. Chem.* **1999**, 2233–2241.

[24] a) M. G. King, G. P. McQuillan, *Inorg. Phys. Theor.* **1967**, 898; b) S. R. Alvarado, I. A. Shortt, H.-J. Fan, J. Vela, *Organometallics* **2015**, *34*, 4023–4031.

[25] a) C. B. Murray, D. J. Norris, M. G. Bawendi, *J. Am. Chem. Soc.* **1993**, *115*, 8706–8715; b) C. Graiff, A. Ienco, C. Massera, C. Mealli, G. Predieri, A. Tiripicchio, F. Ugozzoli, *Inorg. Chem. Acta* **2002**, *330*, 95–102.

[26] a) B. Schmid, L. M. Venanzi, A. Albinati, F. Mathey, *Inorg. Chem.* **1991**, *30*, 4693–4699; b) A. Campos-Carrasco, L. E. E. Broeckx, J. J. M. Weemers, E. A. Pidko, M. Lutz, A. M. Masdeu-Bultó, D. Vogt, C. Müller, *Chem. Eur. J.* **2011**, *17*, 2510–2517; c) A. Loibl, M. Weber, M. Lutz, C. Müller, *Eur. J. Inorg. Chem.* **2019**, 1575–1585; d) I. de Krom, E. A. Pidko, M. Lutz, C. Müller, *Chem. Eur. J.* **2013**, *19*, 7523–7531; e) I. de Krom, L. E. E. Broeckx, M. Lutz, C. Müller, *Chem. Eur. J.* **2013**, *19*, 3676–3684; f) R. J. Newland, M. P. Delve, R. L. Wingad, S. M. Mansell, *New J. Chem.* **2018**, *42*, 19625–19636; g) N. T. Coles, A. S. Abels, J. Leitl, R. Wolf, H. Grützmacher, C. Müller, *Coord. Chem. Rev.* **2021**, *433*, 213729.

[27] S. M. Godfrey, S. L. Jackson, C. A. McAuliffe, R. G. Pritchard, *J. Chem. Soc. Dalton Trans.* **1997**, 4499–4502.

[28] L. Bennett, B. Melchers, B. Proppe, *Curta: A General-purpose High-Performance Computer at ZEDAT, Freie Universität Berlin*, Freie Universität Berlin, **2020**.